



Published in final edited form as:

J Immunol. 2020 April 01; 204(7): 1968–1981. doi:10.4049/jimmunol.1901168.

Osteopontin and iCD8 α cells promote intestinal intraepithelial lymphocyte homeostasis

Ali Nazmi^{*,1}, Michael J. Greer^{†,1}, Kristen L. Hoek^{*,1}, M. Blanca Piazuelo[‡], Joern-Hendrik Weitkamp[§], Danyvid Olivares-Villagómez^{*,¶}

* Department of Pathology, Microbiology and Immunology, Vanderbilt University Medical Center, A5301 Medical Center North, Nashville, Tennessee 37232, USA

† Department of Biomedical Informatics, Vanderbilt University, Nashville, Tennessee, 37232, USA

‡ Department of Medicine, Vanderbilt University Medical Center, 1030 MRBIV, Nashville, Tennessee 37232, USA

§ Department of Pediatrics, Vanderbilt University Medical Center, Monroe Carell Jr. Children's Hospital, 111114 Doctor's Office Tower, Nashville, Tennessee 37232, USA

¶ Vanderbilt Institute for Infection, Immunology and Inflammation, Vanderbilt University Medical Center, A5301 Medical Center North, Nashville, Tennessee 37232, USA

Abstract

Intestinal intraepithelial lymphocytes (IEL) comprise a diverse population of cells residing in the epithelium at the interface between the intestinal lumen and the sterile environment of the lamina propria. Because of this anatomical location, IEL are considered critical components of intestinal immune responses. Indeed, IEL are involved in many different immunological processes ranging from pathogen control to tissue stability. However, despite their critical importance in mucosal immune responses, very little is known about the homeostasis of different IEL subpopulations. The phosphoprotein osteopontin is important for critical physiological processes, including cellular immune responses such as survival of Th17 cells and homeostasis of NK cells, among others. Because of its impact in the immune system, we investigated the role of osteopontin in the homeostasis of IEL. Here, we report that mice deficient in the expression of osteopontin exhibit reduced numbers of the IEL subpopulations TCR $\gamma\delta^+$, TCR β^+ CD4 $^+$, TCR β^+ CD4 $^+$ CD8 α^+ and TCR β^+ CD8 $\alpha\alpha^+$ cells in comparison to wild-type mice. For some IEL subpopulations the decrease in cells numbers could be attributed to apoptosis and reduced cell division. Moreover, we show *in vitro* that exogenous osteopontin stimulates the survival of murine IEL subpopulations and unfractionated IEL derived from human intestines, an effect mediated by CD44, a known osteopontin receptor. We also show that iCD8 α IEL, but not TCR $\gamma\delta^+$ IEL, TCR β^+ IEL or intestinal epithelial cells, can promote survival of different IEL populations via osteopontin, indicating an important role for iCD8 α cells in the homeostasis of IEL.

Corresponding author: Danyvid Olivares-Villagómez, Department of Pathology, Microbiology and Immunology, Vanderbilt University Medical Center, A5301 Medical Center North, Nashville, Tennessee 37232, USA. Telephone, 615-936-0134. Fax, 615-343-7392., danyvid.olivares-villagomez@vumc.org.

¹These authors contributed equally to this report

Introduction

One of the largest immunological compartments in the body is comprised of intraepithelial lymphocytes (IEL), a group of immune cells interspaced between the monolayer of intestinal epithelial cells (IEC). IEL can be divided into two groups based on T cell receptor (TCR) expression (1–3). TCR⁺ IEL express $\alpha\beta$ or $\gamma\delta$ chains. TCR $\alpha\beta$ ⁺ IEL can be further subdivided into TCR $\alpha\beta$ ⁺CD4⁺, TCR $\alpha\beta$ ⁺CD4⁺CD8 $\alpha\alpha$ ⁺, TCR $\alpha\beta$ ⁺CD8 $\alpha\alpha$ ⁺, and TCR $\alpha\beta$ ⁺CD8 $\alpha\beta$ ⁺ cells. TCR^{neg} IEL comprise innate lymphoid cells (ILC) (4–6) and lymphocytes characterized by expression of intracellular CD3 γ chains (iCD3⁺), some of which express CD8 $\alpha\alpha$ (iCD8 α cells) (7, 8).

Because of their anatomical location, IEL function as sentinels between the antigenic contents of the intestinal lumen and the sterile environment under the basal membrane of the epithelium. Indeed, TCR $\gamma\delta$ IEL surveil for pathogens (9), secrete antimicrobials conferring protection against pathobionts (10), and protect from intestinal inflammation (11). Other IEL, like conventional CD8 T cells that migrate into the epithelium, can protect against *Toxoplasma* infection (12) and reside in this organ as memory cells (13, 14). TCR $\alpha\beta$ ⁺CD4⁺CD8 $\alpha\alpha$ ⁺ IEL can prevent development of disease in the T cell adoptive transfer model of colitis (15). iCD8 α cells confer protection against *Citrobacter rodentium* infection and may protect against necrotizing enterocolitis in neonates (8), but these cells can also promote intestinal inflammation in some experimental conditions (16). iCD3⁺ IEL are involved in malignances associated with celiac disease (7).

Osteopontin is a glycosylated phosphoprotein encoded by the Spp-1 (secreted phosphoprotein) gene, originally characterized as part of the rat bone matrix (17, 18). Osteopontin is a versatile molecule involved in many physiological and disease processes (19–21). The role of osteopontin in intestinal inflammation is diverse. For example, Spp-1-deficient mice present with milder disease in the trinitrobenzene sulphonic acid and DSS models of colitis (22, 23). In humans with inflammatory bowel diseases (IBD), plasma osteopontin is significantly increased compared to healthy individuals (24, 25). Some reports indicate that osteopontin is downregulated in the mucosa of Crohn's disease (CD) patients (26), whereas other groups have reported higher osteopontin expression in the intestines of individuals with CD and ulcerative colitis (UC) compared with healthy controls (25, 27). Because of its involvement in IBD, this molecule could be a potential biomarker (28) and has been explored as a therapeutic target in clinical trials (29). These reports clearly underscore the importance of osteopontin in intestinal inflammation and warrant further investigation of this molecule in mucosal immune responses.

Studies of osteopontin in the immune system have provided important insight into the role of this molecule. For example, osteopontin is involved in macrophage chemotaxis (30), inhibition of NK cell apoptosis and promotion of NK cell responses (31), as well as modulation of dendritic cell function (32). In terms of T cells, osteopontin has been shown to stimulate the survival of concanavalin A-activated lymph node T cells *in vitro*, to promote the survival of anti-myelin specific T cells in the central nervous system (33), and to stimulate Th1 responses (34). However, because IEL are different from “conventional” T cells, and have varied and distinct developmental pathways and functions specialized for the

environment of the intestinal epithelium (3), what has been investigated for T cells in other anatomical compartments may not directly translate to IEL, underscoring the need to investigate the role of osteopontin in this peculiar immune site. What we know about the role of osteopontin and IEL homeostasis is very limited. For example, it was reported that the frequency and numbers of TCR $\gamma\delta^+$ IEL were reduced in osteopontin-deficient mice, while unfractionated TCR $\alpha\beta^+$ IEL numbers remained similar in comparison to wild type controls (35). However, *in vitro* neutralization of IEL-derived osteopontin resulted in decreased survival of TCR $\gamma\delta$ and TCR $\alpha\beta$ IEL (35), confounding the *in vivo* results. Our group has recently shown that iCD8 α IEL enhance the survival of ILC1-like IEL, via osteopontin, impacting the development of intestinal inflammation (36). Here, we hypothesize that osteopontin and iCD8 α cells are key components involved in the homeostasis of most IEL populations. In the present report, we investigated this hypothesis by carefully studying the role of osteopontin in the homeostasis of different IEL subpopulations in mice and total IEL derived from human tissue. We present data showing that osteopontin differentially influences the survival, proliferation and migration of distinct IEL subpopulations, and that these effects are mediated in part by one of the many osteopontin ligands, CD44. Furthermore, we show that IEL survival is mediated primarily by iCD8 α cell-derived osteopontin, whereas other TCR $\gamma\delta^+$ and TCR β^+ IEL do not contribute, at least *in vitro*, to the survival of IEL. Moreover, our *in vivo* experiments show that IEC-derived osteopontin do not seem to promote IEL survival. Finally, we present evidence of the impact of osteopontin in the development of intestinal inflammation.

Material and methods

Mice

C57BL/6J were originally purchased from The Jackson Laboratory (000664) and have been maintained and acclimated in our colony for several years. CD44 $^{-/-}$ (005085), CD45.1 (002014), RFP-Foxp3 (008374) and Spp-1 $^{-/-}$ (004936) mice on the C57BL/6 background were originally purchased from The Jackson Laboratory. Rag-2 $^{-/-}$ mice on the C57BL/6 background were provided by Dr. Luc Van Kaer. Spp-1 $^{-/-}$, CD44 $^{-/-}$, and Rag-2 $^{-/-}$ mice were crossed with C57BL/6J wild-type mice to generate heterozygous offspring, and subsequently bred among themselves to generate mutant mice. For co-housing experiments, same sex WT C57BL/6 and Spp-1 $^{-/-}$ mice were co-housed immediately after weaning for a period of 5 weeks. Vill-Cre $^{+/-}$ mice were provided by the laboratory of Dr. Keith Wilson. Spp-1 $^{fl/fl}$ mice on the C57BL/6J background were generated by the Vanderbilt Transgenic Mouse/ES Cell Shared Resource following an established protocol (37). Briefly, intron 1/2 and intron 3/4 of the Spp-1 gene were targeted for insertion of LoxP sites by CRISPR/Cas9 ribonucleoproteins (RNP) along with a 1528 bp megamer symmetrical donor ssDNA oligonucleotide (IDT). crRNA sequences were 5'-GTGTGATAACACAGACTCAT-3' and 5'-AACCAGTACCTTACATGTT-3'. Vill-Cre $^{+/-}$ -Spp-1 $^{fl/fl}$ and Vill-Cre $^{-/-}$ -Spp-1 $^{fl/fl}$ littermate mice were generated by crossing Vill-Cre $^{+/-}$ mice and Spp-1 $^{fl/fl}$ mice. Spp-1 $^{-/-}$ -Rag-2 $^{-/-}$ mice were generated in our colony by breeding Spp-1 $^{+/-}$ with Rag-2 $^{+/-}$ mice. Male and female mice were used for all experiments. Mice were maintained in accordance with the Institutional Animal Care and Use Committee at Vanderbilt University.

Lymphocyte isolation

IEL were isolated by mechanical disruption as previously reported (38). Briefly, after flushing the intestinal contents with cold HBSS and removing excess mucus, the intestines were cut into small pieces (~1 cm long) and shaken for 45 minutes at 37°C in HBSS supplemented with 5% fetal bovine serum and 2 mM EDTA. Supernatants were recovered and cells isolated using a discontinuous 40/70% Percoll (General Electric) gradient. To obtain lamina propria lymphocytes, intestinal tissue was recovered and digested with collagenase (187.5 U/ml, Sigma) and DNase I (0.6 U/ml, Sigma). Cells were isolated using a discontinuous 40/70% Percoll gradient. Spleen and thymus cells were isolated by conventional procedures.

Human samples

The Vanderbilt University Medical Center Institutional Review Board approved sample collection (IRB# 090161 and 190182). Peripheral blood mononuclear cells were isolated by ficoll gradient from unidentified healthy adult volunteers as previously described (39). A pathologist from the Vanderbilt Children's Hospital provided de-identified fresh intestinal tissue specimens from infants. Isolation of human cells associated with the intestinal epithelium was performed as previously described (40). Briefly, tissue was cut in small ~1 cm pieces and incubated with slow shaking for 30 minutes at room temperature in HBSS (without calcium and magnesium) supplemented with 5% fetal bovine serum, 5mM EDTA and 1% antibiotic mix (pen-strep-AmphoB; Fisher-Lonza). After incubation, cells in the supernatant were recovered.

Reagents and flow cytometry

Fluorochrome-coupled anti-mouse CD4 (GK1.5), CD5 (53-7.3), CD25 (PC61.5), CD44 (1M7), CD45 (30F11), CD45.1 (A20), CD45.2 (104), CD8 α (53-6.7), CD8 β (REA793 or H35-17.2), CD122 (TM-bl), TCR β (H57-597), TCR $\gamma\delta$ (eBioGL3), Ki69 (solA15), PD-1 (J43.1), and isotype controls were purchased from ThermoFisher, BD Biosciences or Tonbo. Annexin V and 7AAD were purchased from BD Biosciences. All staining samples were acquired using BD FACS Canto II, 4-Laser Fortessa, or 5-Laser LSR II Flow cytometers (BD Biosciences) and data was analyzed using FlowJo software (Tree Star). Cell staining was performed following conventional techniques. Manufacturer's instructions were followed for Annexin V staining; briefly, early apoptotic cells were considered as annexin V⁺7AAD^{neg}, late apoptotic cells or undergoing necrosis as annexin V⁺7AAD⁺, and necrotic cells as annexin V⁻7AAD⁺. FACS sorting was performed using a FACSAria III at the Flow Cytometry Shared Resource at VUMC.

In vitro survival assay

FACS-enriched IEL subpopulations were incubated in a 96-well flat-bottom well plate (Falcon, Fisher Scientific) at a density of 5×10^5 cells/ml in RPMI containing 10% fetal bovine serum. In some groups culture media was supplemented with recombinant osteopontin (2 μ g/ml) (R&D) or anti-CD44 (5 μ g/ml) (ThermoFisher; clone IM7). Cells were cultured in 5% CO₂ at 37°C. At time 0 and every 24 h, an aliquot from the culture was taken to count live cells using trypan blue to exclude dead cells. Percentage of live cells was

calculated in reference to time 0. For human samples, total PBMC or IEL were cultured in the presence or absence of recombinant human osteopontin (2 µg/ml) (R&D) and anti-human-CD44 (5 µg/ml) (Thermofisher; clone IM7).

Co-culture survival assays

CD45⁺ IEL from *Spp-1*^{-/-} mice were positively selected using magnetic beads (Miltenyi) and cultured (1×10⁵ cells/well) in a 96-well flat-bottomed well plate in RPMI complemented with 10% fetal bovine serum, penicillin/streptomycin, HEPES, L-glutamine and β-mercaptoethanol. These are “read out” cells. Then, these cells were cultured in the presence (1×10⁵ cells/well) or absence of magnetic bead-enriched (Miltenyi) iCD8α cells from *Rag-2*^{-/-} mice, or TCRβ⁺ or TCRγδ⁺ IEL from CD45.1 WT mice. For normalization purposes, the purity of these cells was determined by flow cytometry. Anti-osteopontin antibodies (2 µg/ml) (R&D; clone AF808) were added to some wells. After 4 h of incubation, cells were recovered and stained for surface markers, 7AAD and Annexin V. For all experiments, IEL were gated according to their size in a forward versus side scatter. Then, cells were selected by their expression of CD45.2 and gated for the individual subpopulations, followed by analysis of 7AAD incorporation and annexin V staining. Increased survival was determined as 100 - [% of annexin V⁺ read-out cells in co-culture × 100 / % of annexin V⁺ cells cultured alone]. Osteopontin concentration from these cultures was determined by an ELISA kit (R&D) following the manufacturer’s instructions.

Adoptive transfer of total T cells

Total splenocytes from WT mice were depleted of CD19-positive cells using magnetic beads (Miltenyi). Four to 6 million cells were adoptively transferred (i.p.) into *Rag-2*^{-/-} or *Spp-1*^{-/-}*Rag-2*^{-/-} mice (similar results were observed regardless of the number of cells transferred). Starting weight was determined prior to injection. Seven or 28 days later, recipient mice were weighed, sacrificed and donor cells from the intestines analyzed by flow cytometry. In some experiments a segment of the colon was excised and prepared for histological examination. In some experiments CD19-depleted splenocytes from *CD44*^{-/-} mice were adoptively transferred into *Rag-2*^{-/-} or *Spp-1*^{-/-}*Rag-2*^{-/-} mice. Mice were weighed weekly for 4 weeks, and cells and colon analyzed as indicated above. Pathological evaluation of the colons was done in a blind fashion by Dr. Piauzelo, following established parameters (41).

In vitro and in vivo Foxp3 expression

Lamina propria lymphocytes isolated from RFP-Foxp3 mice were cultured in the presence or absence of recombinant osteopontin and anti-CD44 antibodies as described above. At time 0 and 72 h later, cells were analyzed by flow cytometry to detect RFP expression in live TCR⁺CD4⁺ cells. For *in vivo* experiments, CD4⁺RFP⁺ splenocytes were enriched by FACS and 2 × 10⁵ cells were adoptively transferred i.p. into *Rag-2*^{-/-} or *Spp-1*^{-/-}*Rag-2*^{-/-} mice. Eight weeks later, IEL were isolated and RFP expression analyzed in CD45⁺TCRβ⁺CD4⁺ donor-derived cells.

Transcription profile analysis

For gene expression array, RNA was isolated from FACS-enriched IEL subpopulations from 4 individual WT and *Spp-1^{-/-}* mice. Samples were prepared for RT² Profiler PCR Array (QIAGEN PAMM-012Z) and analyzed following manufacturer's instructions. For RNAseq analysis, RNA was isolated from FACS-enriched CD45⁺ IEL derived from WT mice cultured for 24 h in the presence or absence of recombinant osteopontin using the QIAGEN RNeasy micro kit. Sequencing was performed on an Illumina NovaSeq 6000 (2 × 150 base pair, paired-end reads). The tool Salmon (42) was used for quantifying the expression of RNA transcripts. The R project software along with the edgeR method (43) was used for differential expression analysis. For gene set enrichment analysis (GSEA), RNAseq data was ranked according to the t-test statistic. The gene sets curated (C2), GO (C5), immunological signature collection (C7) and hallmarks of cancer (H) of the Molecular Signatures Database (MSigDB) were used for enrichment analysis. GSEA enrichment plots were generated using the GSEA software (44) from the Broad Institute with 1000 permutations.

Real time PCR for osteopontin expression

RNA from colon tissue was isolated using Trizol following the manufacturer's instructions. First strand cDNA was synthesized using RT2 first strand kit (Qiagen). Real time PCR was performed using RT2 SYBR Green Mastermix (Qiagen). Osteopontin and GAPDH primers were from Qiagen.

Statistical analysis

Statistical significance between 2 groups was determined using Mann-Whitney U-test. For analysis of 3 groups or more, two-way ANOVA followed by Dunn's multiple comparison tests were used appropriately. All data was analyzed in GraphPad Prism 7 and shown as mean ± standard error mean (SEM). A *P* value <0.05 was considered significant.

Results

Osteopontin deficiency has a differential effect on the homeostasis of individual IEL populations

A previous report has shown that mice deficient in osteopontin (*Spp-1^{-/-}*) have reduced TCR $\gamma\delta$ ⁺ total cell numbers in the small intestine, while unfractionated TCR $\alpha\beta$ ⁺ IEL numbers remained the same (35). In the same report, *in vitro* experiments showed that the survival of both of these IEL populations was decreased when cultured in the presence of anti-osteopontin antibodies (35). To further investigate, we analyzed in detail the IEL compartment of WT and *Spp-1^{-/-}* mice. Fig. 1A depicts the gating strategy used. Our analysis showed a decrease in TCR $\gamma\delta$ ⁺ small intestine IEL, but contrary to the report by Ito et al (35), we observed that *Spp-1^{-/-}* mice presented significant reduction in the total numbers of total TCR β ⁺ cells and IEL subpopulations TCR β ⁺CD4⁺, TCR β ⁺CD8 α ⁺ (which includes CD8 $\alpha\beta$ ⁺ and CD8 $\alpha\alpha$ ⁺), and TCR β ⁺CD4⁺CD8 α ⁺ in comparison to cells derived from WT mice (Fig. 1B, top rows). IEL deficiencies were also observed in the colons of *Spp-1^{-/-}* mice (Fig. 1B bottom rows). TCR^{neg} and iCD8 α IEL, presented similar total cell numbers in the small intestine of *Spp-1^{-/-}* and WT mice but reduced numbers in the colons

of *Spp-1*^{-/-} mice (Fig. 1B). Similar results were obtained from co-housed WT and *Spp-1*^{-/-} mice, indicating that osteopontin deficiency is the main contributing factor to the observed IEL deficiency, while other factors, such as the microbiome, do not have a substantial role (Supplemental Fig. 1A). Further subdivision of TCRβ⁺CD8α⁺ IEL based on CD8β expression, showed reduction in small intestine TCRβ⁺CD8αα⁺ and TCRβ⁺CD8αβ⁺ IEL numbers in *Spp-1*^{-/-} mice (Supplemental Fig. 1B and 1C). In the colon, while the number of TCRβCD8αβ⁺ IEL were similar between WT and *Spp-1*^{-/-} mice, there was a significant reduction in the total cell numbers of TCRβ⁺CD8αα⁺ IEL in *Spp-1*^{-/-} mice (Supplemental Fig. 1B and 1C). To determine whether the reduction observed in TCRβ⁺CD8αα⁺ IEL was due to a decrease in their precursor cells, we analyzed WT and *Spp-1*^{-/-} thymocytes. Thymic precursors, defined as CD25^{neg}CD4^{neg}CD8α^{neg}TCRβ⁺CD5⁺CD122⁺ and/or PD-1⁺ cells (45), presented similar cell frequencies between WT and *Spp-1*^{-/-} mice, indicating that the deficiency of TCRβ⁺CD8αα⁺ IEL is not related to a reduction in thymic precursors (Supplemental Fig. 1D).

Interestingly, osteopontin deficiency did not affect spleen T lymphocytes (Fig. 1C) or lamina propria CD19⁺, TCRβ⁺CD4⁺, and TCRβ⁺CD8⁺ cells (Fig. 1D), suggesting that the major influence of this molecule is confined to the intestinal IEL compartment.

To investigate whether the reduction in IEL numbers in *Spp-1*^{-/-} mice was due to increased cell death, we stained the cells with annexin V and 7AAD to determine the levels of early apoptosis (annexin V⁺7AAD^{neg}), late apoptosis/undergoing necrosis (annexin V⁺7AAD⁺) and necrosis (annexin V⁻7AAD⁺). TCRγδ⁺, TCRβ⁺CD4⁺, TCRβ⁺CD4⁺CD8α⁺, TCRβ⁺CD8αα⁺, and TCRβ⁺CD8αβ⁺ IEL derived from *Spp-1*^{-/-} and WT mice presented similar levels of cells in early apoptosis (annexin V⁺7AAD^{neg}) and necrosis (annexin V^{neg}7AAD⁺) (Fig. 2A). On the other hand, TCRγδ⁺, TCRβ⁺CD4⁺, and TCRβ⁺CD4⁺CD8α⁺ IEL derived from *Spp-1*^{-/-} mice presented an increase in cells in late apoptosis/undergoing necrosis (annexin V⁺7AAD⁺), suggesting that the decreased total numbers of these IEL subpopulations in the absence of osteopontin may be due to increased cell death.

We also analyzed the cell division potential of TCRγδ⁺, TCRβ⁺CD4⁺, TCRβ⁺CD4⁺CD8α⁺ and TCRβ⁺CD8αα⁺ and TCRβ⁺CD8αβ⁺ IEL derived from WT and *Spp-1*^{-/-} mice. TCRβ⁺CD4⁺, TCRβ⁺CD4⁺CD8α⁺ and TCRβ⁺CD8αα⁺ IEL from osteopontin-deficient mice presented decreased Ki67 staining in comparison to IEL derived from WT mice (Fig. 2B), indicating lower proliferation of these IEL populations. Interestingly, TCRγδ⁺ IEL had similar Ki67 staining levels in cells from osteopontin-deficient and -competent mice (Fig. 2B).

Overall, these results show that osteopontin is required for proper IEL cell numbers, survival and cell division. Importantly, the effect caused by osteopontin is not homogeneous across most IEL populations, and instead, each IEL population responds differently to this cytokine.

IEL subpopulations survive better in vitro in the presence of osteopontin

To investigate the role of osteopontin in IEL survival, we cultured FACS-enriched TCRγδ⁺, TCRβ⁺CD4⁺, TCRβ⁺CD8α⁺, and TCRβ⁺CD4⁺CD8α⁺ IEL subpopulations in the presence

or absence of recombinant osteopontin, and measured survival every 24 h for a period of 3 days. More than 50% of TCR $\gamma\delta^+$ IEL died after only 24 h of incubation with plain media and continued to die after 48 and 72 h (Fig. 3A). Although TCR $\gamma\delta^+$ IEL incubated in the presence of osteopontin showed cell death during the first 48 h of cultures, their survival at 72 h was higher than cells incubated without recombinant osteopontin (Fig. 3A). A similar increased survival trend was observed for TCR β^+ CD8 α^+ and TCR β^+ CD4 $^+$ CD8 α^+ IEL (Fig. 3A). TCR β^+ CD4 $^+$ IEL were more viable than the other populations at 24 h post culture even without recombinant osteopontin, but addition of this cytokine maintained a constant survival rate of TCR β^+ CD4 $^+$ IEL (Fig. 3A). Osteopontin binds to several integrin receptors including $\alpha\nu\beta 1$, $\alpha\nu\beta 3$, and $\alpha\nu\beta 5$, among others (46), but also interacts with CD44 (47). Staining TCR $\gamma\delta^+$ and unfractionated TCR β^+ IEL from naïve mice with CD44 results in ~80 to 85% CD44 $^+$ cells respectively (Supplemental Fig. 2A). To determine whether the improved survival observed in the presence of osteopontin depends on CD44 binding, IEL subpopulations were incubated in the presence of recombinant osteopontin and anti-CD44 antibody. As shown in Fig. 3A, whenever IEL survival was improved by osteopontin, this effect was blunted by addition of anti-CD44.

To determine whether osteopontin-mediated survival is specific for IEL, we investigated the influence of osteopontin on the survival of splenic T cells. First, CD45 $^+$ splenocytes from naïve WT mice were cultured in the presence or absence of recombinant osteopontin. As shown in Fig. 3B, survival of CD45 $^+$ splenocytes was not affected by osteopontin. Moreover, FACS-enriched TCR β^+ CD44 hi spleen cells from naïve WT and *Spp-1* $^{-/-}$ mice cultured in the presence or absence of recombinant osteopontin and/or anti-CD44 presented no difference in their survival (Fig. 3C), indicating that osteopontin preferentially influences the *in vitro* survival of IEL via CD44 but not of total or CD44 $^+$ splenic T cells.

The immune system of mice maintained in specific pathogen-free conditions more closely resembles that of human neonates rather than adults (48). Therefore, to determine whether our findings with murine IEL are relevant to humans, we isolated total IEL from human neonates and cultured them in the presence or absence of recombinant human osteopontin. Human IEL survived better in the presence of recombinant osteopontin than in its absence, and the addition of anti-human CD44 blunted the cytokine effect (Fig. 3D), in parallel to the results observed with mouse IEL. To determine the effect of osteopontin on other human lymphocytes, we employed PBMC from healthy adults, as we were unable to obtain PBMCs from the same neonate individuals for this purpose. As shown in Fig. 3E, PBMC survival was not enhanced or reduced by any of the treatments used, which corroborates an intestinal IEL-specific effect. Overall, our results indicate that in *in vitro* conditions, osteopontin differentially promotes both murine and human IEL survival, an effect that is blunted by blocking its interaction with CD44.

Because anti-CD44 blocked the survival effect mediated by osteopontin, we investigated whether the IEL compartment is disrupted in CD44-deficient mice. In comparison to IEL derived from WT mice, CD44 $^{-/-}$ mice presented reduced TCR neg and TCR β^+ CD4 $^+$ IEL in the small intestines, whereas the colon presented reduction in unfractionated TCR β^+ , TCR neg , TCR β^+ CD4 $^+$, and TCR β^+ CD8 α^+ IEL (Supplementary Fig. 2B).

Osteopontin induces differential anti-apoptotic gene expression in IEL

The previous sections suggest an important role for osteopontin in the survival of different IEL subpopulations. To investigate whether osteopontin induces a survival gene expression profile, we isolated RNA from FACS-enriched TCR $\gamma\delta^+$, TCR β^+ CD4 $^+$, TCR β^+ CD8 α^+ and TCR β^+ CD4 $^+$ CD8 α^+ IEL derived from naïve WT and Spp-1 $^{-/-}$ mice, and determined the expression of genes involved in preventing apoptosis. Comparison of genes expressed in IEL from WT and Spp-1 $^{-/-}$ mice showed that TCR $\gamma\delta^+$ cells from WT animals had more differentially expressed anti-apoptotic genes in comparison to the other IEL populations (Supplemental Fig. 3A and B). TCR β^+ CD8 α^+ IEL presented little differential expression among the anti-apoptotic genes analyzed. On the other hand, TCR β^+ CD4 $^+$ and TCR β^+ CD4 $^+$ CD8 α^+ IEL differentially expressed some of these genes (Supplemental Fig. 3A and B). Birc2, a known inhibitor of apoptosis in malignancies (49), was one of the genes consistently differentially expressed in most IEL analyzed from WT mice, including TCR β^+ CD4 $^+$ CD8 α^+ cells (Supplemental Fig. 3A and B). Overall, these results indicate that osteopontin induces the expression of anti-apoptotic genes, but the gene profile varies between different IEL subpopulations.

Because addition of recombinant osteopontin rescued IEL survival when cultured *in vitro* (Fig. 3A), we interrogated whether addition of this cytokine in cultured wild type IEL modifies their gene expression profile. For this purpose, we cultured FACS-enriched CD45 $^+$ IEL from wild type mice in the presence or absence of osteopontin. Twenty-four hours post-culture, cells were collected, RNA extracted, sequenced and the gene expression profile determined. As recovery of sufficient cells for gene expression profile analysis after 24 h of culture from individual IEL populations was limiting, total CD45 $^+$ IEL were used as an alternative approach. Gene set enrichment analysis (GSEA) revealed that IEL cultured in the presence of recombinant osteopontin express genes associated with retinoid X receptor (RXR) functions (Supplemental Fig. 3C and D). GSEA also showed that IEL cultured in media alone present enriched pathways related to apoptosis, degradation of p27/p21 and downregulation of genes in regulatory T cells (Supplemental Fig. 3C and D). These results indicate that *in vitro* IEL exposure to osteopontin has an impact on IEL gene transcription and modifies gene sets related to cell survival.

Osteopontin does not influence T cell migration into the epithelium but maintains homeostasis of TCR β^+ CD4 $^+$ and TCR β^+ CD4 $^+$ CD8 α^+ IEL

Because some IEL populations are derived from conventional CD4 $^+$ and CD8 $^+$ T cells, we investigated whether osteopontin is important for the relocation of these cells into the IEL compartment. To test this hypothesis, we adoptively transferred total spleen T cells from WT mice into Rag-2 $^{-/-}$ or Spp-1 $^{-/-}$ Rag-2 $^{-/-}$ recipient mice, and after 7 days we determined the number of cells migrating into the intestinal epithelium. Fig. 4A (top) shows the gating strategy to identify cells derived from donor mice. Both TCR β^+ CD4 $^+$ and TCR β^+ CD8 α^+ cells migrated similarly into the epithelium of Rag-2 $^{-/-}$ or Spp-1 $^{-/-}$ Rag-2 $^{-/-}$ recipient mice (Fig. 4A, bottom), indicating that osteopontin in the recipient mice does not influence the migration of these cells into the intestinal mucosa. Interestingly, reconstitution analysis of Spp-1 $^{-/-}$ Rag-2 $^{-/-}$ recipient mice at 28 days post transfer showed a reduction in the total number of TCR β^+ CD4 $^+$ and TCR β^+ CD4 $^+$ CD8 α^+ cells but not TCR β^+ CD8 α^+ IEL (Fig.

4B), which resembled what was observed in naïve *Spp-1*-deficient mice (Fig. 1B). To prevent the development of intestinal inflammation in *Rag-2*^{-/-} recipient mice, we transferred total T cells, which includes regulatory T cells. To our surprise, *Spp-1*^{-/-}*Rag-2*^{-/-} recipient mice lost more weight than *Rag-2*^{-/-} mice (Fig. 4C) and presented increased colon inflammation (Fig. 4D). The impact of osteopontin produced by donor-derived cells in IEL reconstitution and disease development was minimal, as determined by total colon osteopontin mRNA expression prior to, and after 28 days post T cell transfer (Fig. 4E).

To interrogate why *Spp-1*^{-/-}*Rag-2*^{-/-} mice developed intestinal inflammation when regulatory T cells were present in the inoculum, we investigated the fate of regulatory T cells in the presence or absence of osteopontin. Regulatory T cells are known to express CD44, which when ligated, promotes sustained Foxp3 expression (50). Thus, we hypothesized that binding of osteopontin to CD44 is a potential signal that maintains proper Foxp3 expression. To test this possibility, we cultured total T cells from the intestines of RFP-Foxp3 mice in the presence or absence of osteopontin, with or without anti-CD44. After 72 h of culture, there was an increase in the percentage of RFP⁺ cells in the presence of osteopontin, which was blunted with the addition of anti-CD44 antibodies (Fig. 5A). Figure 5B shows the combined fold increase over untreated cells.

To test whether osteopontin sustains Foxp3 expression *in vivo*, we sorted splenic RFP⁺ cells from RFP-Foxp3 reporter mice and adoptively transferred them into *Rag-2*^{-/-} or *Spp-1*^{-/-}*Rag-2*^{-/-} recipient mice. Eight weeks after transfer, IEL were isolated and the percentage of donor-derived (CD45⁺TCRβ⁺CD4⁺) RFP⁺ cells was determined (Fig. 5C). *Rag-2*^{-/-} mice presented a trend of higher percentage of donor-derived cells in the IEL compartment than *Spp-1*^{-/-}*Rag-2*^{-/-} recipient mice (Fig. 5D). Approximately 10% of the donor-derived cells from *Rag-2*^{-/-} recipient mice remained RFP⁺, whereas only 4% of cells recovered from *Spp-1*^{-/-}*Rag-2*^{-/-} recipient mice remained RFP⁺ (Fig. 5E). These results indicate that osteopontin sustains Foxp3 expression in regulatory T cells in the IEL compartment, possibly mediated by CD44 ligation, which significantly impacts the development of intestinal inflammation.

To test whether CD44 expression, as one of the receptors for osteopontin on T cells, is critical for prevention of experimental colitis, we adoptively transferred total T cells from *CD44*^{-/-} donor mice into *Rag-2*^{-/-} and *Spp-1*^{-/-}*Rag-2*^{-/-} recipient mice. *Rag-2*^{-/-} mice that received total spleen T cells from WT mice did not lose weight, whereas *Rag-2*^{-/-} and *Spp-1*^{-/-}*Rag-2*^{-/-} recipient mice that received spleen cells from *CD44*^{-/-} donor mice lost weight comparably starting at 2 weeks post transfer (Supplemental Fig. 3E), with clear signs of intestinal inflammation (Supplemental Fig. 3F).

Overall, these results show that osteopontin is not involved in the migration of adoptively transferred conventional T cells into the intestinal epithelium, but sustains proper TCRβ⁺CD4⁺ and TCRβ⁺CD4⁺CD8⁺ cell numbers once in the IEL compartment. Moreover, the lack of osteopontin in recipient mice results in development of colitis, even in the presence of regulatory T cells in the inoculum. A similar outcome was observed when *CD44*-deficient

T cells were transferred into Rag-2^{-/-} or Spp-1^{-/-}Rag-2^{-/-} recipient mice, highlighting the importance of the osteopontin-CD44 interaction in intestinal homeostasis.

iCD8 α cell-derived osteopontin increases IEL survival

iCD8 α cells are a population of TCR^{neg} IEL involved in different immunological roles and are known as an important source of osteopontin in the intestines (8). Recently, it has been shown that survival of TCR^{neg} ILC1-like IEL depends in part on iCD8 α cells, an effect most likely associated with the production of osteopontin by these cells (36). To determine whether the survival of TCR⁺ IEL populations is dependent on iCD8 α cell-derived osteopontin, we performed experiments in which the source of osteopontin is confined to a specific IEL population (iCD8 α , TCR β ⁺ or TCR $\gamma\delta$ ⁺ cells). Then, these individual IEL populations were co-cultured in the presence of total IEL derived from osteopontin-deficient mice. After 4 h of culture, cells were stained for annexin V and the increase in survival was calculated as indicated in the Materials and methods section. As shown in Fig. 6A, addition of osteopontin-competent iCD8 α cells to the IEL culture resulted in an increased survival (over IEL cultured in the absence of iCD8 α cells) of almost 30% for TCR $\gamma\delta$ ⁺ and TCR β ⁺CD8 $\alpha\alpha$ ⁺ IEL, whereas there was variable survival increase for unfractionated TCR β ⁺, and the IEL subpopulations TCR β ⁺CD4⁺, TCR β ⁺CD4⁺CD8 α ⁺ and TCR β ⁺CD8 $\alpha\beta$ ⁺. Survival was reduced by addition of anti-osteopontin antibodies, indicating that iCD8 α cell-derived osteopontin was responsible for the observed increase in survival. A previous report indicated that TCR β ⁺ and TCR $\gamma\delta$ ⁺ IEL also produce osteopontin (35). To determine whether these IEL populations promote *in vitro* survival of IEL, we performed a similar experiment but the potential source of osteopontin were TCR β ⁺ or TCR $\gamma\delta$ ⁺ IEL (Fig. 6B and C). TCR β ⁺ IEL were capable of stimulating survival of only TCR $\gamma\delta$ ⁺ IEL and addition of anti-osteopontin antibodies blunted the survival below the levels of cells cultured alone (Fig. 6B). For other IEL population, the addition of TCR β ⁺ IEL from osteopontin-competent mice did not enhance IEL survival (Fig. 6B). When TCR $\gamma\delta$ ⁺ IEL were used as the source of osteopontin, these cells were capable of increasing only the survival of TCR β ⁺CD8 $\alpha\beta$ ⁺ IEL. To determine that the osteopontin-competent cells have similar viability after 4 h of culture, we analyzed their annexin V profile. As indicated in Supplemental Fig. 4A, iCD8 α , TCR β ⁺ and TCR $\gamma\delta$ ⁺ IEL presented low percentage of annexin V-positive cells, and these percentages were similar among the 3 different type of IEL. To determine the production of osteopontin from each cell type in these co-cultures, we recovered the supernatants and measured osteopontin concentration by ELISA. As expected, osteopontin was not detected in supernatants from CD45⁺ IEL derived from Spp-1^{-/-} mice cultured alone, but was readily detectable in cultures containing iCD8 α cells (Supplemental Fig. 4B). On the other hand, osteopontin was not detected in the supernatants that included TCR β ⁺ or TCR $\gamma\delta$ ⁺ IEL from osteopontin-competent mice (Supplemental Fig. 4B). These results suggest that the observed increased survival promoted by TCR β ⁺ and TCR $\gamma\delta$ ⁺ IEL may not be completely dependent on osteopontin, since this protein was not detected in the supernatants. Overall, these results indicate that iCD8 α cell-derived osteopontin is an important survival signal for IEL.

Intestinal epithelial cells are known to constitutively express low levels of osteopontin (25, 26), representing a potential source of this protein for the homeostasis of IEL. Because IEC rapidly die in *in vitro* culture conditions, we determine their contribution to IEL homeostasis

by analyzing the IEL compartment of mice with conditional mutation of the osteopontin gene driven by the villin promoter, which is preferentially expressed in IEC (Vill.Cre^{+/-}Spp-1^{fl/fl}). Expression of osteopontin in IEC is ablated in Vill.Cre^{+/-}Spp-1^{fl/fl} mice, but not in activated T cells, validating the conditional mutation (Supplemental Fig. 4C). As shown in Fig. 7A and B, the absence of osteopontin expression in IEC does not impact total small intestine or colon IEL cell numbers, indicating that IEC-derived osteopontin does not contribute to the homeostasis of most IEL populations.

Discussion

Intestinal IEL reside in the unique environment of the IEC monolayer. In this anatomical location, IEL are poised as one of the first immunological defenses against potential pathogens from the intestinal lumen. In order to fulfill their immunological roles, IEL need to maintain their homeostasis. However, because IEL represent a diverse population of lymphoid cells, requirements for their homeostasis within the epithelium may depend on the particular type of IEL. For example, TCR $\gamma\delta^+$ IEL require IL-7 for their proper development whereas other IEL are not affected by this cytokine (51). On the other hand, IL-15 deficiency does not disturb TCR $\gamma\delta^+$ IEL but has a significant impact on TCR $\alpha\beta^+$ CD8 α^+ , iCD8 α and iCD3⁺ IEL (7, 8, 52). The results presented in this report indicate that osteopontin is important for the homeostasis of many different IEL subpopulations. This implies that despite having different developmental pathways and cytokine requirements, the presence of osteopontin in the epithelium ensures proper homeostasis of most types of intestinal IEL.

Osteopontin-mediated T cell survival has been documented previously. For example, concanavalin A-activated T cells from lymph nodes show reduced levels of cell death in the presence of osteopontin (33). It is important to note that this report demonstrated a pivotal role for osteopontin as an enhancer for the survival of effector Th17 cells, particularly during brain inflammation (33). However, whereas this group studied differentiated Th17 cells in the context of brain inflammation our results are based on IEL in naïve animals. In the present report, using an *in vitro* system, we show that TCR⁺ IEL rapidly die in the absence of osteopontin, whereas the presence of this cytokine increased their *in vitro* survival (Fig. 3). Interestingly, each IEL subpopulation presented different survival kinetics, but appeared to have a similar survival requirement for osteopontin. Strikingly, the effect of osteopontin was only observed at 48 h (TCR β^+ CD4⁺ and TCR β CD4⁺CD8 α^+ IEL) or 72 h (TCR $\gamma\delta^+$ and TCR β^+ CD8 α^+ IEL). The reason why the osteopontin effect is only observed at later time points and not at 24 h is not clear. However, it is possible that as IEL are exposed to exogenous osteopontin during the first hours of culture, there is a decrease in their annexin V profile (as shown in Fig. 6), however their resilience to cell death is delayed, which is observed at later time points.

CD44 is known to be one of the receptors for osteopontin, and the interaction between these two molecules promotes adhesion and chemotaxis of bone marrow cells (53), increases growth of cancer cell lines (54), stimulates survival of pro-B cell lines (55), induces production of IL-10 in T cells (56), and protects T cell hybridomas from activated-induced cell death (57), among other functions. Despite the many roles attributed to the osteopontin-CD44 interaction, its role in IEL survival has not been investigated. IEL are considered to be

in a “semi-activated” state (58), and most of these cells express CD44. Therefore, it is reasonable to speculate that some IEL subpopulations receive survival signals via the interaction between osteopontin and CD44. Interestingly, splenic CD44⁺ T cell survival was not increased by the addition of osteopontin *in vitro*, which suggests that osteopontin may not affect all T cells expressing CD44. We also show that the IEL survival promoted by osteopontin can be blunted by addition of anti-CD44 antibodies (Fig. 3), underscoring the importance of the osteopontin-CD44 interaction in IEL biology. However, it is noteworthy that IEL deficiencies in CD44^{-/-} mice do not faithfully resemble those observed in Spp-1^{-/-} mice, suggesting that in the absence of CD44, other receptors may bind osteopontin to stimulate survival of specific IEL subpopulations.

In the adoptive transfer experiments reported here, donor CD4 T cells from WT mice reconstituted the IEL compartment of Spp-1^{-/-}Rag-2^{-/-} recipient mice less efficiently than in Rag-2^{-/-} recipient mice, suggesting that an environment capable of producing osteopontin is important for proper cell reconstitution in the intestines. However, transfer of T cells from osteopontin-deficient donor mice into Rag-2^{-/-} recipient mice resulted in reduced survival rates in the spleen and lymph nodes in comparison to donor T cells from wild type donor mice (31). These results indicate that intrinsic T cell-derived osteopontin is critical for normal cell reconstitution in secondary lymphoid organs whereas T cells present in the IEL compartment depend on osteopontin from the environment.

Adoptive transfer of total spleen T cells into immunodeficient hosts, such as Rag-2^{-/-} mice, normally results in cellular reconstitution and protection from T cell-mediated colitis due to the presence of regulatory T cells (59, 60). Surprisingly, when recipient Rag-2^{-/-} mice were deficient in osteopontin (Rag-2^{-/-}Spp-1^{-/-} animals), mice developed colitis even in the presence of regulatory T cells (Fig. 4), raising the possibility that environmental osteopontin is important for maintaining regulatory T cell function, as shown in Fig. 5.

If most IEL subpopulations require osteopontin for their homeostasis, what are the cellular sources for this protein in the intestines? IEC produce osteopontin, and its expression increases during inflammation (25, 26). Other sources of osteopontin are within the IEL compartment, which appear to be confined to IEL expressing CD8 α , including TCR $\gamma\delta$ ⁺, TCR β ⁺, and iCD8 α cells (8, 35). We have previously shown that the survival of TCR^{neg} ILC1-like IEL (NKp46⁺NK1.1⁺) depends on iCD8 α cell-derived osteopontin (36). Our previous publication and the results presented herein provide significance evidence to suggest that one of the main roles for iCD8 α cells is the maintenance of proper IEL homeostasis. iCD8 α cells constitute around 2 to 5% of the total IEL compartment. Considering that IEL are interspaced between IEC at an approximate ratio of 1 IEL for 10 IEC (2), how do iCD8 α cells promote osteopontin-dependent survival of IEL in the monolayer of intestinal epithelial cells? It is known that some IEL, like TCR $\gamma\delta$ ⁺ cells scan the intestinal epithelium by moving out through the basal section of the epithelium and entering the IEC monolayer in another location (61). Therefore, it is possible that iCD8 α cells use a similar mechanism to scan the monolayer, reach other IEL and provide needed osteopontin to other cells.

In the past few years, the role of osteopontin in the etiology of human diseases has been greatly appreciated. For example, recent work has investigated the use of neutralizing anti-osteopontin antibodies as a therapeutic with preclinical studies currently underway (ref. in (62)). Studies such as the one described herein show that osteopontin neutralization may affect IEL homeostasis in individuals with non-gastrointestinal tract disorders, but may be beneficial for IBD patients. Osteopontin appears to be a critical molecule with multiple effects, one of them supporting proper IEL homeostasis, and therefore additional studies are needed to better understand its function and how it affects the biology of the mucosal immune system.

Supplementary Material

Refer to Web version on PubMed Central for supplementary material.

Acknowledgments

We thank the Flow Cytometry Shared Resource for technical help and guidance; the Translational Pathology Shared Resource for tissue processing; the Vanderbilt Genome Editing Resource, especially Dr. Leesa Sampson for her outstanding help for the generation of the *Spp-1^{fl/fl}* mice. We are thankful to Theresa Rogers, RN, for her help securing human blood and tissue samples. We thank Dr. Luc Van Kaer for reviewing the manuscript

This work was supported by NIH grant R01DK111671 (D.O-V.); Careers in Immunology Fellowship Program from the American Association of Immunologists (D.O-V. and A.N.); National Library of Medicine T15 LM00745 grant (M.J.G); scholarships from the Digestive Disease Research Center at Vanderbilt University Medical Center supported by NIH grant P30DK058404; and the Vanderbilt Genome Editing Resource supported by a Diabetes Research and Training Center Grant (DK020593) and Cancer Center Support Grant (CA68485)

References

1. Cheroutre H, Lambolez F, and Mucida D. 2011 The light and dark sides of intestinal intraepithelial lymphocytes. *Nat Rev Immunol* 11: 445–456. [PubMed: 21681197]
2. Olivares-Villagomez D, and Van Kaer L. 2017 Intestinal Intraepithelial Lymphocytes: Sentinels of the Mucosal Barrier. *Trends Immunol.*
3. Van Kaer L, and Olivares-Villagomez D. 2018 Development, Homeostasis, and Functions of Intestinal Intraepithelial Lymphocytes. *J Immunol* 200: 2235–2244. [PubMed: 29555677]
4. Fuchs A, Vermi W, Lee JS, Lonardi S, Gilfillan S, Newberry RD, Cella M, and Colonna M. 2013 Intraepithelial type 1 innate lymphoid cells are a unique subset of IL-12- and IL-15-responsive IFN- γ -producing cells. *Immunity* 38: 769–781. [PubMed: 23453631]
5. Talayero P, Mancebo E, Calvo-Pulido J, Rodriguez-Munoz S, Bernardo I, Laguna-Goya R, Cano-Romero FL, Garcia-Sesma A, Loinaz C, Jimenez C, Justo I, and Paz-Artal E. 2016 Innate Lymphoid Cells Groups 1 and 3 in the Epithelial Compartment of Functional Human Intestinal Allografts. *Am J Transplant* 16: 72–82. [PubMed: 26317573]
6. Van Acker A, Gronke K, Biswas A, Martens L, Saeys Y, Filtjens J, Taveirne S, Van Ammel E, Kerre T, Matthys P, Taghon T, Vandekerckhove B, Plum J, Dunay IR, Diefenbach A, and Leclercq G. 2017 A Murine Intestinal Intraepithelial Nkp46-Negative Innate Lymphoid Cell Population Characterized by Group 1 Properties. *Cell Rep* 19: 1431–1443. [PubMed: 28514662]
7. Eittersperger J, Montcuquet N, Malamut G, Guegan N, Lopez-Lastra S, Gayraud S, Reimann C, Vidal E, Cagnard N, Villarese P, Andre-Schmutz I, Gomes Domingues R, Godinho-Silva C, Veiga-Fernandes H, Lhermitte L, Asnafi V, Macintyre E, Cellier C, Beldjord K, Di Santo JP, Cerf-Bensussan N, and Meresse B. 2016 Interleukin-15-Dependent T-Cell-like Innate Intraepithelial Lymphocytes Develop in the Intestine and Transform into Lymphomas in Celiac Disease. *Immunity* 45: 610–625. [PubMed: 27612641]
8. Van Kaer L, Algood HM, Singh K, Parekh VV, Greer MJ, Piazzuelo MB, Weitkamp JH, Matta P, Chaturvedi R, Wilson KT, and Olivares-Villagomez D. 2014 CD8 α α (+) Innate-Type

Lymphocytes in the Intestinal Epithelium Mediate Mucosal Immunity. *Immunity* 41: 451–464. [PubMed: 25220211]

9. Edelblum KL, Singh G, Odenwald MA, Lingaraju A, El Bissati K, McLeod R, Sperling AI, and Turner JR. 2015 gammadelta Intraepithelial Lymphocyte Migration Limits Transepithelial Pathogen Invasion and Systemic Disease in Mice. *Gastroenterology* 148: 1417–1426. [PubMed: 25747597]
10. Ismail AS, Severson KM, Vaishnav S, Behrendt CL, Yu X, Benjamin JL, Ruhn KA, Hou B, DeFranco AL, Yarovinsky F, and Hooper LV. 2011 Gammadelta intraepithelial lymphocytes are essential mediators of host-microbial homeostasis at the intestinal mucosal surface. *Proc Natl Acad Sci U S A* 108: 8743–8748. [PubMed: 21555560]
11. Inagaki-Ohara K, Chinen T, Matsuzaki G, Sasaki A, Sakamoto Y, Hiromatsu K, Nakamura-Uchiyama F, Nawa Y, and Yoshimura A. 2004 Mucosal T cells bearing TCRgammadelta play a protective role in intestinal inflammation. *J Immunol* 173: 1390–1398. [PubMed: 15240735]
12. Lepage AC, Buzoni-Gatel D, Bout DT, and Kasper LH. 1998 Gut-derived intraepithelial lymphocytes induce long term immunity against *Toxoplasma gondii*. *J Immunol* 161: 4902–4908. [PubMed: 9794424]
13. Masopust D, Choo D, Vezys V, Wherry EJ, Duraiswamy J, Akondy R, Wang J, Casey KA, Barber DL, Kawamura KS, Fraser KA, Webby RJ, Brinkmann V, Butcher EC, Newell KA, and Ahmed R. 2010 Dynamic T cell migration program provides resident memory within intestinal epithelium. *J Exp Med* 207: 553–564. [PubMed: 20156972]
14. Masopust D, Jiang J, Shen H, and Lefrancois L. 2001 Direct analysis of the dynamics of the intestinal mucosa CD8 T cell response to systemic virus infection. *J Immunol* 166: 2348–2356. [PubMed: 11160292]
15. Das G, Augustine MM, Das J, Bottomly K, Ray P, and Ray A. 2003 An important regulatory role for CD4+CD8 alpha alpha T cells in the intestinal epithelial layer in the prevention of inflammatory bowel disease. *Proc Natl Acad Sci U S A* 100: 5324–5329. PMC1535703. [PubMed: 12695566]
16. Kumar AA, Delgado AG, Piazuolo MB, Van Kaer L, and Olivares-Villagomez D. 2017 Innate CD8alphaalpa(+) lymphocytes enhance anti-CD40 antibody-mediated colitis in mice. *Immun Inflamm Dis* 5: 109–123. [PubMed: 28474503]
17. Franzen A, and Heinegard D. 1985 Isolation and characterization of two sialoproteins present only in bone calcified matrix. *Biochem J* 232: 715–724. [PubMed: 4091817]
18. Prince CW, Oosawa T, Butler WT, Tomana M, Bhowan AS, Bhowan M, and Schrohenloher RE. 1987 Isolation, characterization, and biosynthesis of a phosphorylated glycoprotein from rat bone. *J Biol Chem* 262: 2900–2907. [PubMed: 3469201]
19. Di Bartolomeo M, Pietrantonio F, Pellegrielli A, Martinetti A, Mariani L, Daidone MG, Bajetta E, Pelosi G, de Braud F, Floriani I, and Miceli R. 2016 Osteopontin, E-cadherin, and beta-catenin expression as prognostic biomarkers in patients with radically resected gastric cancer. *Gastric Cancer* 19: 412–420. [PubMed: 25862567]
20. Giachelli CM, Bae N, Almeida M, Denhardt DT, Alpers CE, and Schwartz SM. 1993 Osteopontin is elevated during neointima formation in rat arteries and is a novel component of human atherosclerotic plaques. *J Clin Invest* 92: 1686–1696. [PubMed: 8408622]
21. Icer MA, and Gezmen-Karadag M. 2018 The multiple functions and mechanisms of osteopontin. *Clin Biochem* 59: 17–24. [PubMed: 30003880]
22. Oz HS, Zhong J, and de Villiers WJ. 2012 Osteopontin ablation attenuates progression of colitis in TNBS model. *Dig Dis Sci* 57: 1554–1561. [PubMed: 22173746]
23. Zhong J, Eckhardt ER, Oz HS, Bruemmer D, and de Villiers WJ. 2006 Osteopontin deficiency protects mice from Dextran sodium sulfate-induced colitis. *Inflamm Bowel Dis* 12: 790–796. [PubMed: 16917234]
24. Mishima R, Takeshima F, Sawai T, Ohba K, Ohnita K, Isomoto H, Omagari K, Mizuta Y, Ozono Y, and Kohno S. 2007 High plasma osteopontin levels in patients with inflammatory bowel disease. *J Clin Gastroenterol* 41: 167–172. [PubMed: 17245215]
25. Sato T, Nakai T, Tamura N, Okamoto S, Matsuoka K, Sakuraba A, Fukushima T, Uede T, and Hibi T. 2005 Osteopontin/Eta-1 upregulated in Crohn's disease regulates the Th1 immune response. *Gut* 54: 1254–1262. [PubMed: 16099792]

26. Gassler N, Autschbach F, Gauer S, Bohn J, Sido B, Otto HF, Geiger H, and Obermuller N. 2002 Expression of osteopontin (Eta-1) in Crohn disease of the terminal ileum. *Scand J Gastroenterol* 37: 1286–1295. [PubMed: 12465727]
27. Masuda H, Takahashi Y, Asai S, and Takayama T. 2003 Distinct gene expression of osteopontin in patients with ulcerative colitis. *J Surg Res* 111: 85–90. [PubMed: 12842452]
28. Neuman MG 2012 Osteopontin biomarker in inflammatory bowel disease, animal models and target for drug discovery. *Dig Dis Sci* 57: 1430–1431. [PubMed: 22410852]
29. Boumans MJ, Houbiers JG, Verschuere P, Ishikura H, Westhovens R, Brouwer E, Rojkovich B, Kelly S, den Adel M, Isaacs J, Jacobs H, Gomez-Reino J, Holtkamp GM, Hastings A, Gerlag DM, and Tak PP. 2012 Safety, tolerability, pharmacokinetics, pharmacodynamics and efficacy of the monoclonal antibody ASK8007 blocking osteopontin in patients with rheumatoid arthritis: a randomised, placebo controlled, proof-of-concept study. *Annals of the rheumatic diseases* 71: 180–185. [PubMed: 21917822]
30. Lund SA, Wilson CL, Raines EW, Tang J, Giachelli CM, and Scatena M. 2013 Osteopontin mediates macrophage chemotaxis via alpha4 and alpha9 integrins and survival via the alpha4 integrin. *J Cell Biochem* 114: 1194–1202. [PubMed: 23192608]
31. Leavenworth JW, Verbinnen B, Wang Q, Shen E, and Cantor H. 2015 Intracellular osteopontin regulates homeostasis and function of natural killer cells. *Proc Natl Acad Sci U S A* 112: 494–499. [PubMed: 25550515]
32. Shinohara ML, Kim HJ, Kim JH, Garcia VA, and Cantor H. 2008 Alternative translation of osteopontin generates intracellular and secreted isoforms that mediate distinct biological activities in dendritic cells. *Proc Natl Acad Sci U S A* 105: 7235–7239. [PubMed: 18480255]
33. Hur EM, Youssef S, Haws ME, Zhang SY, Sobel RA, and Steinman L. 2007 Osteopontin-induced relapse and progression of autoimmune brain disease through enhanced survival of activated T cells. *Nat Immunol* 8: 74–83. [PubMed: 17143274]
34. Ashkar S, Weber GF, Panoutsakopoulou V, Sanchirico ME, Jansson M, Zawaideh S, Rittling SR, Denhardt DT, Glimcher MJ, and Cantor H. 2000 Eta-1 (osteopontin): an early component of type-1 (cell-mediated) immunity. *Science* 287: 860–864. [PubMed: 10657301]
35. Ito K, Nakajima A, Fukushima Y, Suzuki K, Sakamoto K, Hamazaki Y, Ogasawara K, Minato N, and Hattori M. 2017 The potential role of Osteopontin in the maintenance of commensal bacteria homeostasis in the intestine. *PLoS One* 12: e0173629. [PubMed: 28296922]
36. Nazmi A, Hoek KL, Greer MJ, Piazuolo MB, Minato N, and Olivares-Villagomez D. 2019 Innate CD8alphaalpha+ cells promote ILC1-like intraepithelial lymphocyte homeostasis and intestinal inflammation. *PLoS One* 14: e0215883. [PubMed: 31291255]
37. Quadros RM, Miura H, Harms DW, Akatsuka H, Sato T, Aida T, Redder R, Richardson GP, Inagaki Y, Sakai D, Buckley SM, Seshacharyulu P, Batra SK, Behlke MA, Zeiner SA, Jacobi AM, Izu Y, Thoreson WB, Urness LD, Mansour SL, Ohtsuka M, and Gurumurthy CB. 2017 Easi-CRISPR: a robust method for one-step generation of mice carrying conditional and insertion alleles using long ssDNA donors and CRISPR ribonucleoproteins. *Genome biology* 18: 92. [PubMed: 28511701]
38. Olivares-Villagomez D, Mendez-Fernandez YV, Parekh VV, Lalani S, Vincent TL, Cheroutre H, and Van Kaer L. 2008 Thymus leukemia antigen controls intraepithelial lymphocyte function and inflammatory bowel disease. *Proc Natl Acad Sci U S A* 105: 17931–17936. PMC2584730. [PubMed: 19004778]
39. Hoek KL, Samir P, Howard LM, Niu X, Prasad N, Galassie A, Liu Q, Allos TM, Floyd KA, Guo Y, Shyr Y, Levy SE, Joyce S, Edwards KM, and Link AJ. 2015 A cell-based systems biology assessment of human blood to monitor immune responses after influenza vaccination. *PLoS One* 10: e0118528. [PubMed: 25706537]
40. Weitkamp JH, Koyama T, Rock MT, Correa H, Goettel JA, Matta P, Oswald-Richter K, Rosen MJ, Engelhardt BG, Moore DJ, and Polk DB. 2013 Necrotising enterocolitis is characterised by disrupted immune regulation and diminished mucosal regulatory (FOXP3)/effector (CD4, CD8) T cell ratios. *Gut* 62: 73–82. [PubMed: 22267598]
41. Aranda R, Sydora BC, McAllister PL, Binder SW, Yang HY, Targan SR, and Kronenberg M. 1997 Analysis of intestinal lymphocytes in mouse colitis mediated by transfer of CD4+, CD45RBhigh T cells to SCID recipients. *J Immunol* 158: 3464–3473. [PubMed: 9120308]

42. Patro R, Duggal G, Love MI, Irizarry RA, and Kingsford C. 2017 Salmon provides fast and bias-aware quantification of transcript expression. *Nature methods* 14: 417–419. [PubMed: 28263959]
43. Robinson MD, McCarthy DJ, and Smyth GK. 2010 edgeR: a Bioconductor package for differential expression analysis of digital gene expression data. *Bioinformatics* 26: 139–140. [PubMed: 19910308]
44. Subramanian A, Tamayo P, Mootha VK, Mukherjee S, Ebert BL, Gillette MA, Paulovich A, Pomeroy SL, Golub TR, Lander ES, and Mesirov JP. 2005 Gene set enrichment analysis: a knowledge-based approach for interpreting genome-wide expression profiles. *Proc Natl Acad Sci U S A* 102: 15545–15550. [PubMed: 16199517]
45. Ruscher R, Kummer RL, Lee YJ, Jameson SC, and Hogquist KA. 2017 CD8 α intraepithelial lymphocytes arise from two main thymic precursors. *Nat Immunol* 18: 771–779. [PubMed: 28530714]
46. Yokosaki Y, Tanaka K, Higashikawa F, Yamashita K, and Eboshida A. 2005 Distinct structural requirements for binding of the integrins α 6 β 1, α 3 β 1, α 5 β 1 and α 9 β 1 to osteopontin. *Matrix biology : journal of the International Society for Matrix Biology* 24: 418–427. [PubMed: 16005200]
47. Katagiri YU, Sleeman J, Fujii H, Herrlich P, Hotta H, Tanaka K, Chikuma S, Yagita H, Okumura K, Murakami M, Saiki I, Chambers AF, and Uede T. 1999 CD44 variants but not CD44s cooperate with β 1-containing integrins to permit cells to bind to osteopontin independently of arginine-glycine-aspartic acid, thereby stimulating cell motility and chemotaxis. *Cancer Res* 59: 219–226. [PubMed: 9892210]
48. Beura LK, Hamilton SE, Bi K, Schenkel JM, Odumade OA, Casey KA, Thompson EA, Fraser KA, Rosato PC, Filali-Mouhim A, Sekaly RP, Jenkins MK, Vezyz V, Haining WN, Jameson SC, and Masopust D. 2016 Normalizing the environment recapitulates adult human immune traits in laboratory mice. *Nature* 532: 512–516. [PubMed: 27096360]
49. Smolewski P, and Robak T. 2011 Inhibitors of apoptosis proteins (IAPs) as potential molecular targets for therapy of hematological malignancies. *Curr Mol Med* 11: 633–649. [PubMed: 21902653]
50. Bollyky PL, Falk BA, Long SA, Preisinger A, Braun KR, Wu RP, Evanko SP, Buckner JH, Wight TN, and Nepom GT. 2009 CD44 costimulation promotes FoxP3⁺ regulatory T cell persistence and function via production of IL-2, IL-10, and TGF- β . *J Immunol* 183: 2232–2241. [PubMed: 19635906]
51. Maki K, Sunaga S, Komagata Y, Kodaira Y, Mabuchi A, Karasuyama H, Yokomuro K, Miyazaki JI, and Ikuta K. 1996 Interleukin 7 receptor-deficient mice lack γ delta T cells. *Proc Natl Acad Sci U S A* 93: 7172–7177. PMC38955. [PubMed: 8692964]
52. Kennedy MK, Glaccum M, Brown SN, Butz EA, Viney JL, Embers M, Matsuki N, Charrier K, Sedger L, Willis CR, Brasel K, Morrissey PJ, Stocking K, Schuh JC, Joyce S, and Peschon JJ. 2000 Reversible defects in natural killer and memory CD8 T cell lineages in interleukin 15-deficient mice. *J Exp Med* 191: 771–780. [PubMed: 10704459]
53. Weber GF, Ashkar S, Glimcher MJ, and Cantor H. 1996 Receptor-ligand interaction between CD44 and osteopontin (Eta-1). *Science* 271: 509–512. [PubMed: 8560266]
54. Sun SJ, Wu CC, Sheu GT, Chang HY, Chen MY, Lin YY, Chuang CY, Hsu SL, and Chang JT. 2016 Integrin β 3 and CD44 levels determine the effects of the OPN- α splicing variant on lung cancer cell growth. *Oncotarget* 7: 55572–55584. [PubMed: 27487131]
55. Lin YH, and Yang-Yen HF. 2001 The osteopontin-CD44 survival signal involves activation of the phosphatidylinositol 3-kinase/Akt signaling pathway. *J Biol Chem* 276: 46024–46030. [PubMed: 11590166]
56. Murugaiyan G, Mittal A, and Weiner HL. 2008 Increased osteopontin expression in dendritic cells amplifies IL-17 production by CD4⁺ T cells in experimental autoimmune encephalomyelitis and in multiple sclerosis. *J Immunol* 181: 7480–7488. [PubMed: 19017937]
57. Larkin J, Renukaradhya GJ, Sriram V, Du W, Gervay-Hague J, and Brutkiewicz RR. 2006 CD44 differentially activates mouse NK T cells and conventional T cells. *J Immunol* 177: 268–279. [PubMed: 16785522]

58. Montufar-Solis D, Garza T, and Klein JR. 2007 T-cell activation in the intestinal mucosa. *Immunol Rev* 215: 189–201. PMC2754816. [PubMed: 17291289]
59. Powrie F, Correa-Oliveira R, Mauze S, and Coffman RL. 1994 Regulatory interactions between CD45RB^{high} and CD45RB^{low} CD4⁺ T cells are important for the balance between protective and pathogenic cell-mediated immunity. *J Exp Med* 179: 589–600. PMC2191378. [PubMed: 7905019]
60. Powrie F, Leach MW, Mauze S, Menon S, Caddle LB, and Coffman RL. 1994 Inhibition of Th1 responses prevents inflammatory bowel disease in scid mice reconstituted with CD45RB^{hi} CD4⁺ T cells. *Immunity* 1: 553–562. [PubMed: 7600284]
61. Hoytema van Konijnenburg DP, Reis BS, Pedicord VA, Farache J, Victora GD, and Mucida D. 2017 Intestinal Epithelial and Intraepithelial T Cell Crosstalk Mediates a Dynamic Response to Infection. *Cell* 171: 783–794 e713. [PubMed: 28942917]
62. Farrokhi V, Chabot JR, Neubert H, and Yang Z. 2018 Assessing the Feasibility of Neutralizing Osteopontin with Various Therapeutic Antibody Modalities. *Sci Rep* 8: 7781. [PubMed: 29773891]

Key Points

1. Osteopontin promotes homeostasis of mouse and human IEL, mediated by its ligand CD44
2. iCD8 α cells produce osteopontin which impacts the survival of other IEL
3. Lack of osteopontin renders mice susceptible to intestinal inflammation

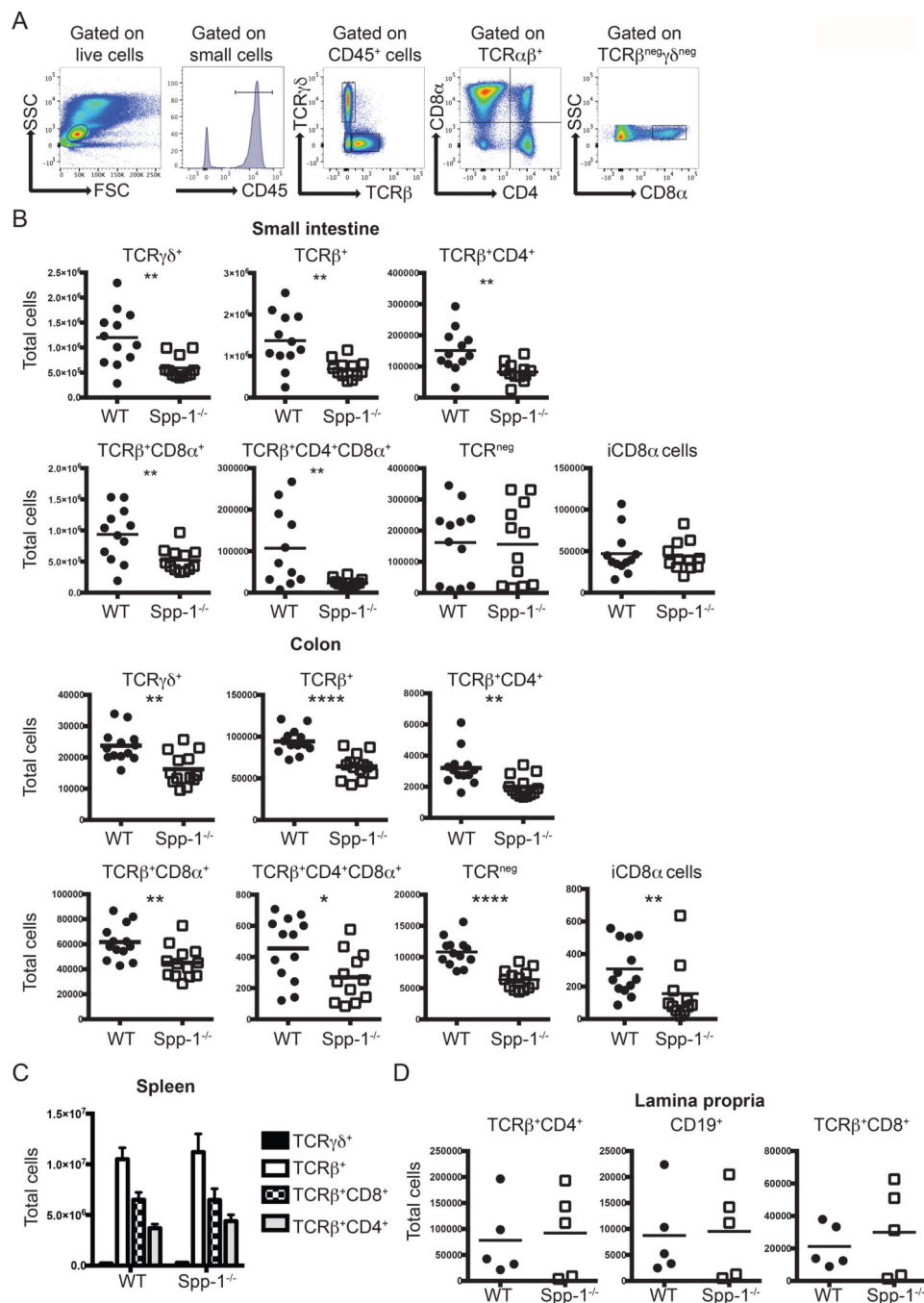


Figure 1. Osteopontin-deficient mice have a reduced IEL compartment. (A) Gating strategy utilized in this report. After gating on live cells, IEL were gated as indicated. (B) Total IEL numbers from the small intestine (top) and colon (bottom) of WT and Spp-1^{-/-} mice. Each dot represents an individual mouse (n = 13). (C) Total cell numbers of the indicated populations in the spleens from WT and Spp-1^{-/-} mice (n = 8). Bars indicate SEM. (D) Total cell numbers of the indicated populations in the lamina propria from WT and Spp-1^{-/-} mice. Each dot represents an individual mouse (n = 5). Data from (B) to (D) are representative of

two to three independent experiments. * $P < 0.05$; ** $P < 0.01$; **** $P < 0.0001$ (Mann-Whitney U test).

Author Manuscript

Author Manuscript

Author Manuscript

Author Manuscript

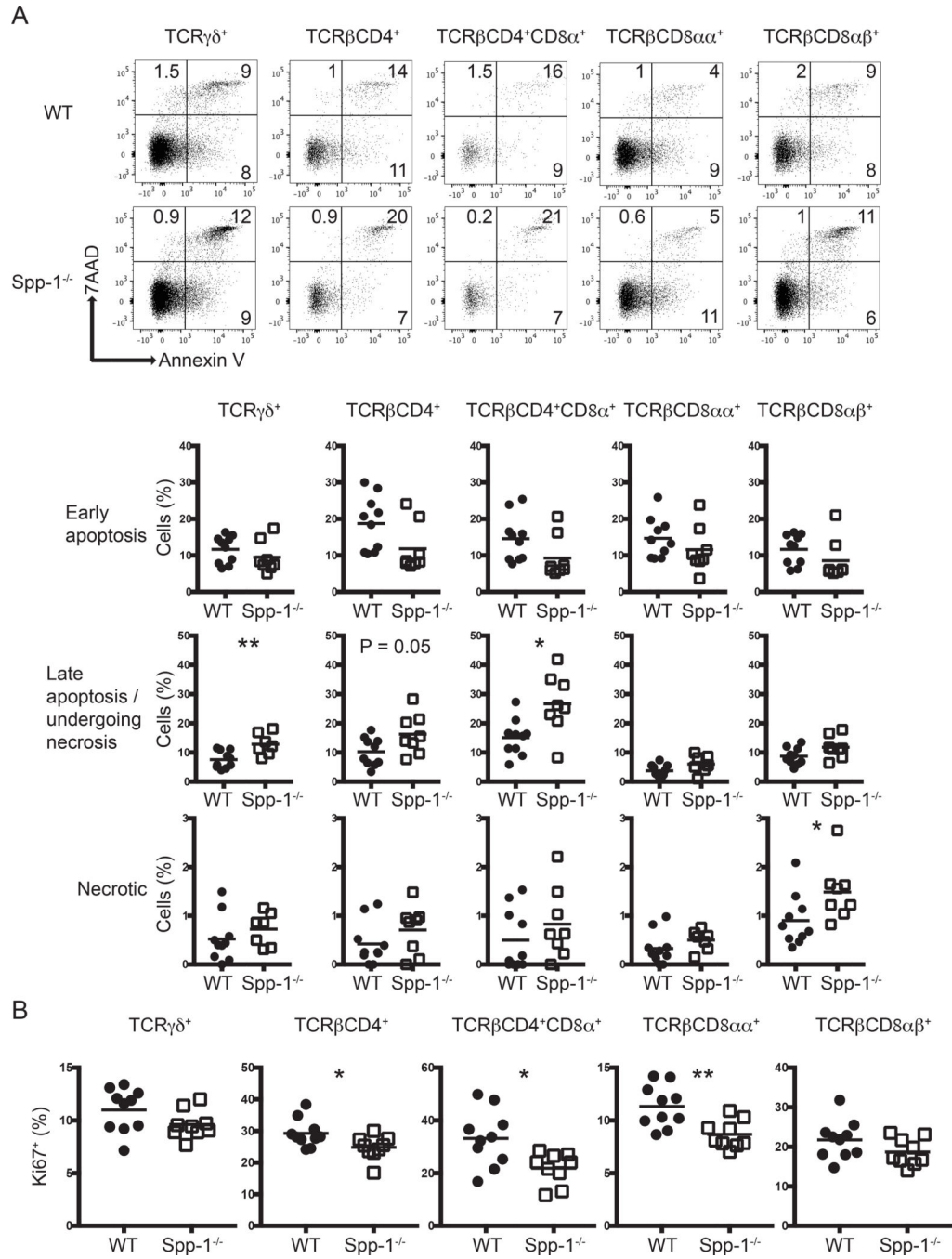


Figure 2. Differential apoptosis and cell division in IEL from osteopontin-deficient mice. (A) Annexin V staining of different small intestine IEL populations derived from WT and Spp-1 $^{-/-}$ mice. After gating cells by size based on forward and side scatter profiles, cells were gated for the expression of CD45 and other surface markers as indicated in Fig. 1A, and then analyzed for annexin V and 7AAD staining. Dot plots show a representative sample. Summary is indicated in the graphs. Data are representative of three independent experiments. Each dot represents an individual sample ($n = 8$ to 10). (B) Ki67 intracellular staining of different

small intestine IEL populations derived from WT and *Spp-1^{-/-}* mice. Cells were gated as in Figure 1A. Data are representative from two independent experiments. Each dot represents an individual sample ($n = 9$ to 10). * $P < 0.05$; ** $P < 0.01$ (Mann-Whitney U test).

Author Manuscript

Author Manuscript

Author Manuscript

Author Manuscript

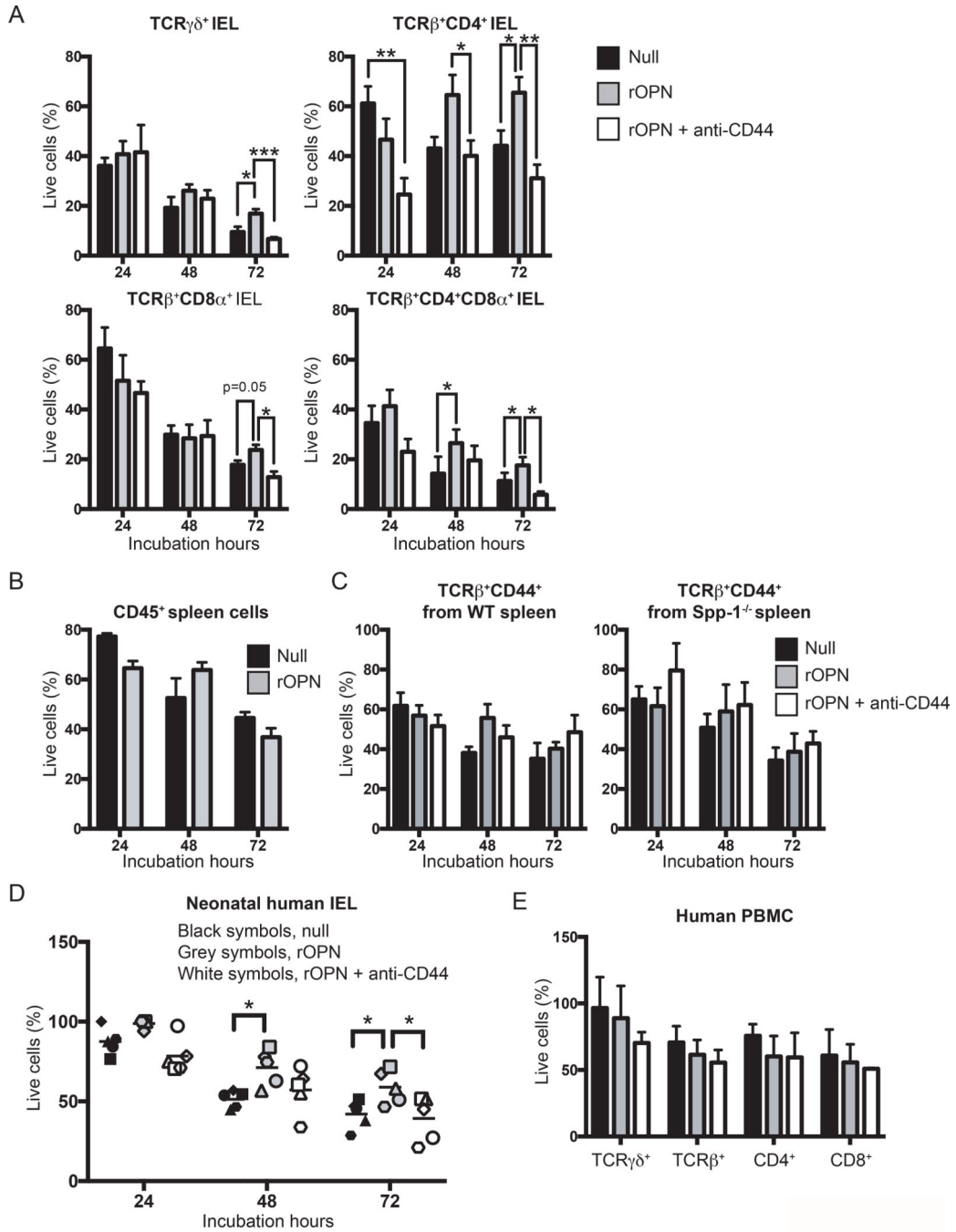


Figure 3. Osteopontin promotes *in vitro* IEL survival. (A) Indicated FACS-enriched IEL populations from WT mice were left untreated or treated with recombinant murine osteopontin (rOPN; 2 μ g/ml), with or without anti-mouse CD44 (5 μ g/ml). After the indicated time points, cell survival was determined. Data are representative of three independent experiments. Biological replicas consisted of two to three pooled IEL preparations from individual mice; each experiment consisted of 3 biological replicas. (B) Enriched CD45⁺ splenocytes were treated as in (A). Data are representative of two independent experiments (n = 3). (C) FACS-

enriched TCR β ⁺CD44⁺ spleen cells from WT and Spp-1^{-/-} mice were treated as in (A). Data are representative of two independent experiments (n = 3). (D) Neonatal human IEL were incubated in the presence or absence of recombinant human osteopontin (2 μ g/ml) and anti-human CD44 (5 μ g/ml). After the indicated time points, cell survival was determined. Each symbol represents an individual human: circle, small intestine from 1-day old patient presenting volvulus and necrosis; square, ileum and colon from 17-day old patient presenting necrotizing enterocolitis; triangle, jejunum from 12-day old patient presenting necrotizing enterocolitis; diamond and hexagon, de-identified individuals. (E) PBMC from adult humans were treated as in (D). Data are representative of two independent experiments (n = 3). **P*<0.05, ***P*<0.01, ****P*<0.001 (One-way ANOVA).

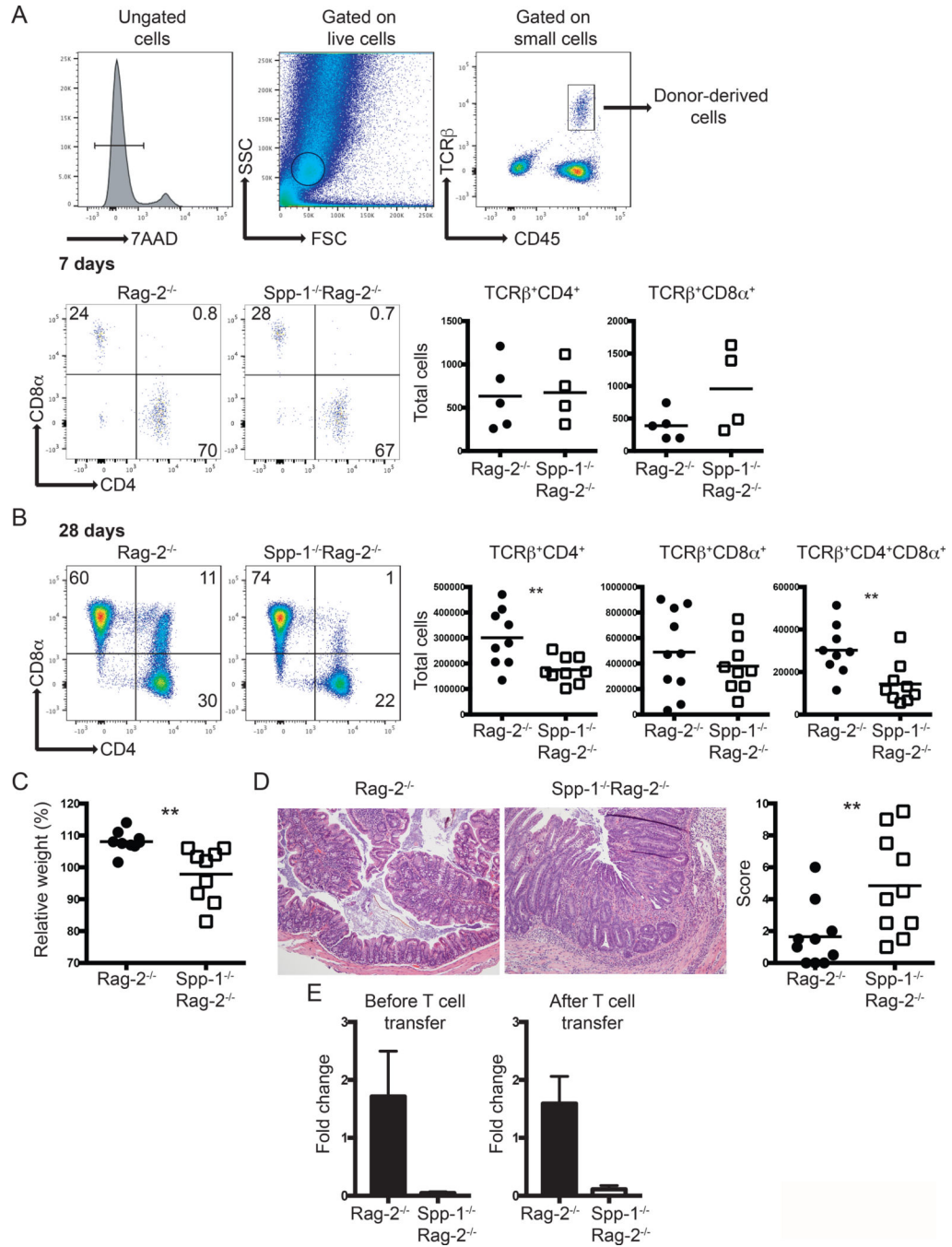


Figure 4. Environmental osteopontin influences IEL reconstitution and colon inflammation. Enriched total spleen T cells from WT mice were adoptively transferred into Rag-2^{-/-} and Spp-1^{-/-}Rag-2^{-/-} mice. (A) Gating strategy to identify cells derived from donor mice (top). Representative analysis of mice analyzed seven days after transfer (bottom). Dot plots show a representative sample. Results are summarized in the graphs. TCRβ⁺CD4⁺CD8α⁺ cells were not detected above background at this time point in either group. Data are representative from two independent experiments. Each dot represents an individual sample

(n = 4 to 5). (B) The same analysis as in (A) performed at 28 days post transfer. Dot plots show a representative sample. Results are summarized in the graphs. Data are representative from three independent experiments. Each dot represents an individual animal (n = 9). (C) Total weight change at 28 days post transfer of mice treated as in (B). (D) Representative H&E stained samples of colon sections from the indicated mice at 28 days (100X magnification). Graph indicates total histological score [immune cell infiltration (3 points), loss of goblet cells (3 points), crypt damage (3 points) and epithelial hyperplasia (3 points)]. For (C) and (D) data are representative from three independent experiments, each dot represents an individual mouse (n = 9). (E) Total mRNA expression from colons of naïve and T cell treated (28 days post-transfer) Rag-2^{-/-} and Spp-1^{-/-}Rag-2^{-/-} mice (n=3–5). ***P*<0.01 (Mann-Whitney T test).

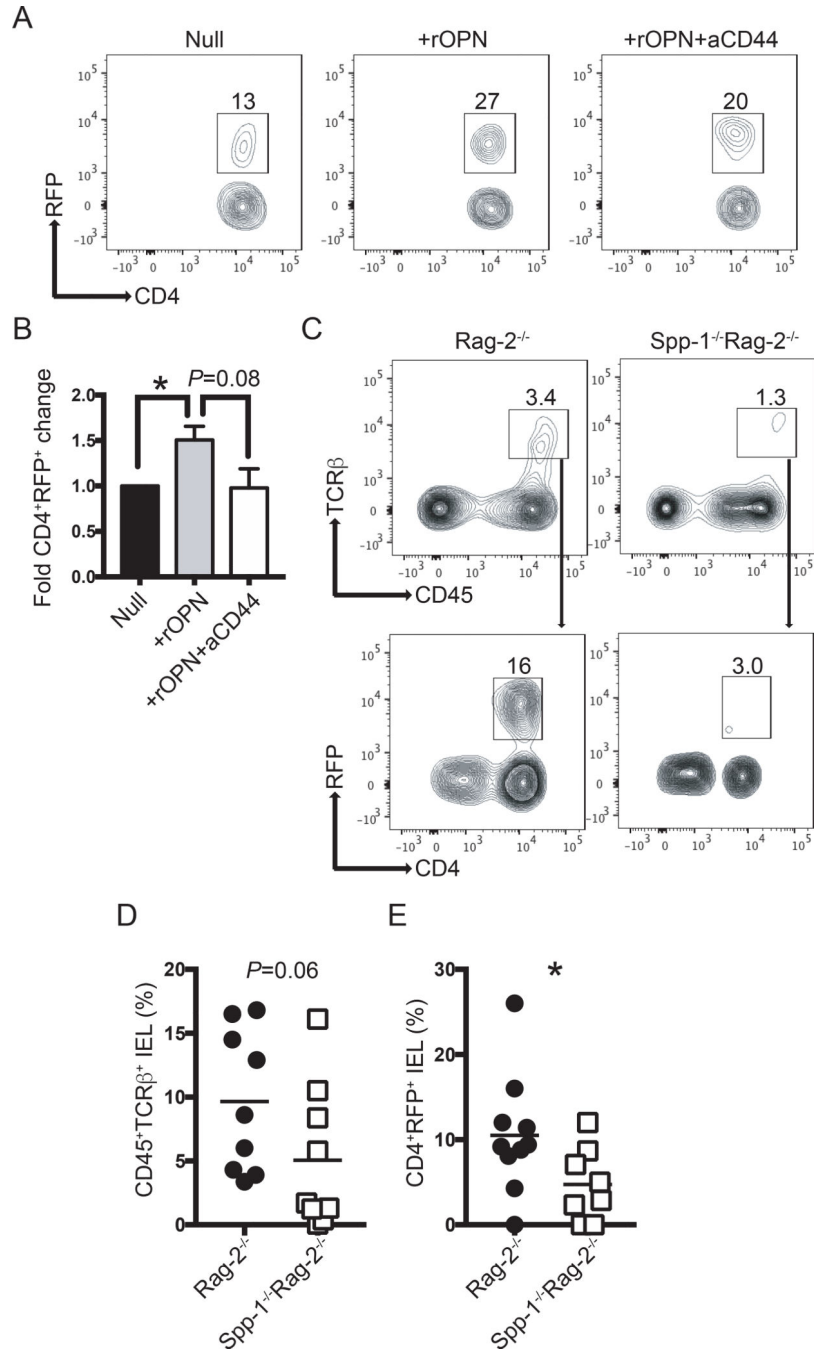


Figure 5. Osteopontin sustains Foxp3 expression. (A) Intestinal T cells from RFP-Foxp3 reporter mice were isolated and cultured in the presence or absence of recombinant osteopontin (2 μg/ml) and anti-CD44 (5 μg/ml). Seventy-two hours later, the percentage of RFP⁺ cells was determined by flow cytometry. After excluding dead cells, dot plots were gated as CD45⁺TCRβ⁺ cells. (B) Bar graph indicates the fold change in CD4⁺RFP⁺ cells in relation to the null group. Data are representative of three independent experiments. (C) Enriched splenic RFP⁺ cells from RFP-Foxp3 reporter mice were adoptively transferred into Rag-2^{-/-}

and *Spp-1*^{-/-}*Rag-2*^{-/-} recipient mice. Eight weeks after transfer, IEL from small intestine were isolated and the percentage of RFP⁺ determined. After excluding dead cells, plots were gated as indicated by the arrows. (D) Summary of the percentage of donor-derived cells recovered; each dot represents an individual mouse. Data are representative from three independent experiments. (E) Summary of the percentage of RFP⁺ cells within the donor-derived cells. **P*<0.05 (Mann-Whitney T test). rOPN = recombinant osteopontin; aCD44 = anti-CD44 antibodies.

Author Manuscript

Author Manuscript

Author Manuscript

Author Manuscript

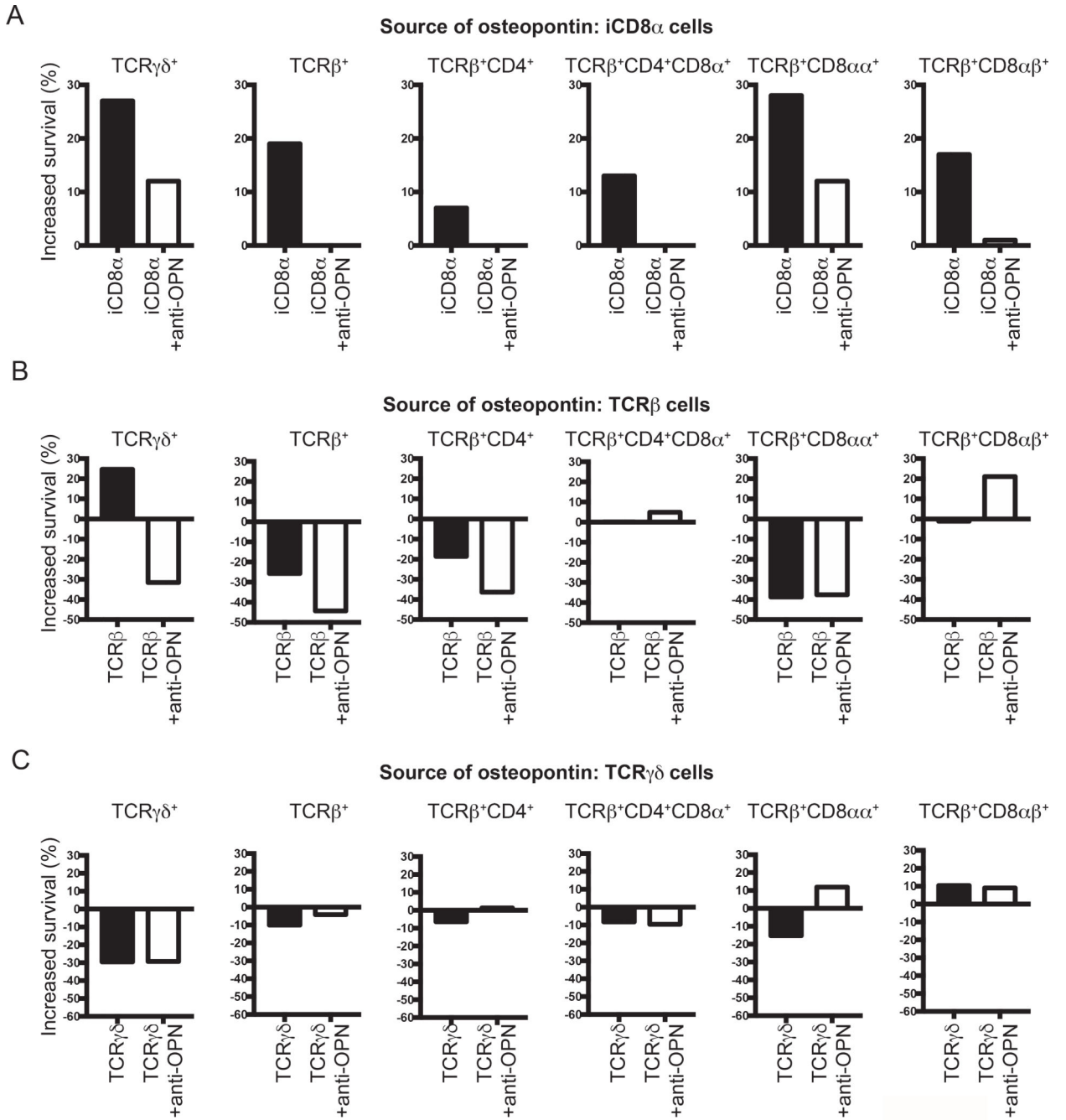


Figure 6. iCD8 α cell-derived osteopontin promotes IEL survival. Enriched CD45 $^+$ IEL from small intestine and colon derived from *Spp-1* $^{-/-}$ mice were incubated in the presence or absence of enriched iCD8 α IEL (A), TCR β^+ IEL (B), or TCR $\gamma\delta^+$ IEL (C) from osteopontin-competent donors. Some cells were cultured in the presence of anti-osteopontin antibodies (2 μ g/ml). Four hours after incubation, cells were stained for surface markers, including annexin V, and 7AAD. Cells were gated as in Figure 2A. Graphs indicate “increased survival”, which was

determined as $100 - [\% \text{ of annexin V}^+ \text{ read-out cells in co-culture} \times 100 / \% \text{ of annexin V}^+ \text{ cells cultured alone}]$.

Author Manuscript

Author Manuscript

Author Manuscript

Author Manuscript

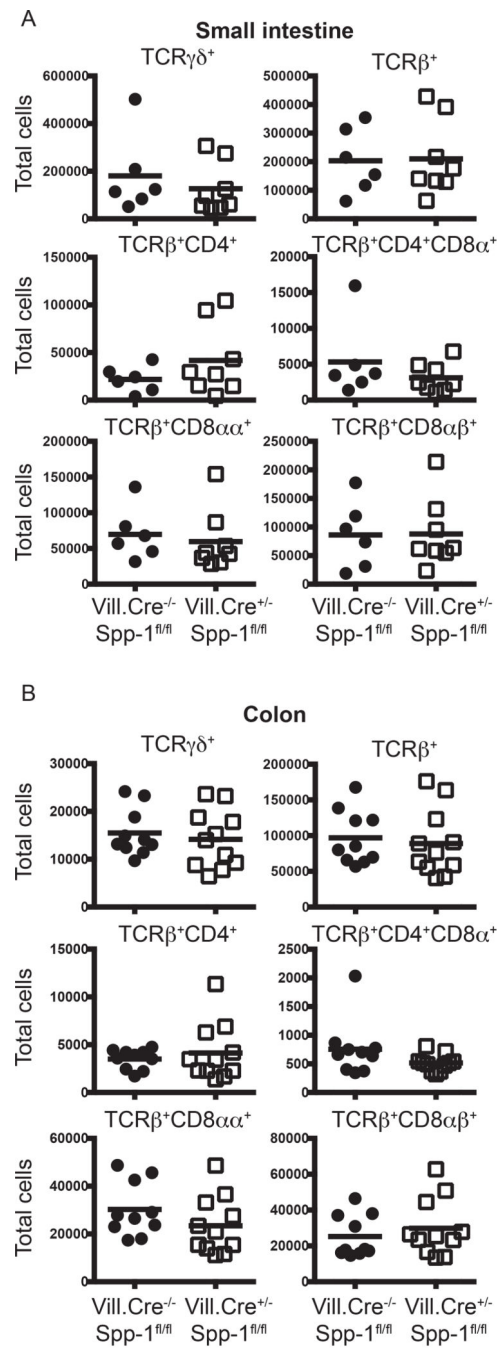


Figure 7. IEC-derived osteopontin does not promote IEL homeostasis. Small intestine (A) and colon (B) IEL were isolated from Villin-Cre^{-/-}Spp-1^{fl/fl} and Villin-Cre^{+/-}Spp-1^{fl/fl} mice, and the cellularity determined as indicated in Fig. 1A and B.